



# The Effect of Promiscuous Aggregation on *in Vitro* Drug Metabolism Assays

Francesco Tres<sup>1</sup> · Maria M. Posada<sup>2</sup> · Stephen D. Hall<sup>2</sup> · Michael A. Mohutsky<sup>2</sup> · Lynne S. Taylor<sup>1</sup>

Received: 30 August 2019 / Accepted: 9 October 2019

© Springer Science+Business Media, LLC, part of Springer Nature 2019

## ABSTRACT

**Purpose** Many bioactive molecules show a type of solution phase behavior, termed promiscuous aggregation, whereby at micromolar concentrations, colloidal drug-rich aggregates are formed in aqueous solution. These aggregates are known to be a major cause of false positives and false negatives in select enzymatic high-throughput screening assays. The goal of this study was to investigate the impact of drug-rich aggregates on *in vitro* drug screening metabolism assays.

**Methods** Cilnidipine was selected as an aggregate former and its impact on drug metabolism was evaluated against rCYP2D6, rCYP1A2, rCYP2C9 and human liver microsomes.

**Results** The cilnidipine aggregates were shown to non-specifically inhibit multiple cytochrome P450 enzymes with an IC<sub>50</sub> comparable with the IC<sub>50</sub> of potent model inhibitors.

**Conclusions** This newly demonstrated mode of “promiscuous inhibition” is of great importance as it can lead to false positives during drug metabolism evaluations and thus it needs to be considered in the future to better predict *in vivo* drug-drug interactions.

**KEY WORDS** Metabolism · non-specific inhibition · promiscuous aggregation

## ABBREVIATIONS

CAC Critical aggregation concentration  
DDI Drug-drug interactions  
HLM Human liver microsomes  
HPLC High performance liquid chromatography

## INTRODUCTION

Many clinically important drug-drug interactions (DDIs) are caused by inhibition of cytochrome P450 enzymes in the liver and intestine (1). Predicting the ability of drug candidates to inhibit cytochrome P450 enzymes on the basis of *in vitro* data generated from human liver microsomes (HLMs) is an essential part of the drug discovery/development process (2–4). While the prediction accuracy for DDIs is often good using these *in vitro* assays, it is poor for some compounds. Poor predictivity can result from inaccurate estimation of the concentration of the inhibitor at the enzyme *in vitro* or *in vivo*, inaccurate estimation of drug binding to the microsomal matrix or plasma, and physical interactions between the compound and the enzymes which result in an artefactual decrease of activity (4,5). Inaccurate prediction of enzyme inhibition is very important as it can lead to unwarranted deprioritization of potential new drugs.

In a high-throughput screen of a large compound library, 95% of the molecules found to act as promiscuous inhibitors were classified as aggregate-based inhibitors (6). The phenomenon of aggregation-based inhibition has been widely reported to lead to false positives during enzyme-based high-throughput screens that are used for drug discovery (6–13). Promiscuous aggregate inhibitors give rise to false positives as they non-specifically inhibit soluble enzymes by sequestration and partial denaturation (8,14). They also show little relationship between structure and activity, and are characterized by poor specificity (15). These colloids have been reported to have a size ranging from 50 to 500 nm in radius, and to have

✉ Lynne S. Taylor  
lstaylor@purdue.edu

<sup>1</sup> Department of Industrial and Physical Pharmacy, College of Pharmacy, Purdue University, West Lafayette, Indiana 47907, USA

<sup>2</sup> Drug Disposition, Lilly Research Laboratories, Eli Lilly and Co., Indianapolis, Indiana 46285, USA

a critical aggregation concentration (CAC) with aggregation reversed by dilution or disrupted by nonionic detergents (8). Colloidal aggregation has been also shown to reduce/eliminate the antiproliferative activity of some drugs, leading to false negatives in cell-based assays (16). This was attributed to the colloids not being able to diffuse through the cell membrane and reach the site of action, when compared to the free drug.

While the phenomenon of promiscuous aggregation-based inhibition has been widely investigated in the context of enzyme-based high-throughput screens, and a number of methods have been employed to identify false positives and false negatives, its impact on *in vitro* drug screening metabolism assays is to date entirely unexplored. In these assays, the metabolism of a well-characterized substrate molecule for a given CYP enzyme is commonly studied in combination with a second new molecular entity (NME) whose inhibition mechanisms are under evaluation (17). If the NME forms drug-rich aggregates, it can be hypothesized that the *in vitro* assessment of enzyme inhibition will be impacted by several potential mechanisms. First, the promiscuous aggregates may sequester hydrophobic substrates, reducing the free concentration and consequently changing the kinetics. The phenomenon of compounds partitioning into aggregates has been previously described for ritonavir, lopinavir, paclitaxel, felodipine (18), atazanavir (19), nifedipine and bicalutamide (20). Second, aggregates can directly interfere with and (partially) denature proteins present in the membranes. This is a non-specific effect that would manifest as inhibition of multiple enzymes. Given these potential phenomena, it is important to evaluate the impact, if any, of aggregate-forming compounds on *in vitro* liver microsomal metabolic assays, with the ultimate goal of improving *in vivo* predictions based on *in vitro* data.

In this study, cilnidipine, a dihydropyridine calcium channel blocker with very low aqueous solubility, was selected as a model aggregate forming compound. Cilnidipine has been previously shown to form colloidal aggregates at low concentrations, approximately 4  $\mu\text{M}$  (21). Tamoxifen, carvedilol, phenacetin and diclofenac were used as probe compounds that are substrates for different CYP enzymes, and the metabolic activity of various recombinant CYPs and human liver microsomes (HLM) was evaluated in the absence and presence of cilnidipine drug-rich aggregates. The chemical structures of the compounds used are reported in Fig. 1. Enzyme kinetic data were complemented by ultracentrifugation measurements to investigate the potential partitioning of the probe compound into the aggregates, and light scattering measurements to determine the onset concentration for the formation of drug-rich cilnidipine aggregates in the presence of microsomes.

## EXPERIMENTAL SECTION

### Materials

Cilnidipine was purchased from Euroasia (Mumbai, India) and Selleck Chemicals (Houston, TX). Tamoxifen and phenacetin were purchased from Sigma-Aldrich Corp. (St. Louis, MO). Carvedilol was obtained from Attix Pharmaceuticals (Montreal, Canada) and Sigma-Aldrich Corp. (St. Louis, MO). Diclofenac was purchased from Spectrum Chemical (New Brunswick, NJ) and Sigma-Aldrich Corp. (St. Louis, MO). Phenacetin,  $\beta$ -NADPH were obtained from Sigma-Aldrich Corp. (St. Louis, MO). Hydroxybufuralol, acetaminophen, 4-hydroxydiclofenac and all stable labelled internal standards were obtained from Cerilliant (Round Rock, TX). Pooled Sprague Dawley rat liver microsomes (male) were obtained from XenoTech (Kansas City, MO). Human liver microsomes (mixed gender) and recombinant CYP enzymes were obtained from Corning (Woburn, MA).

### METHODS

#### Formation of Drug-Rich Aggregates in the Presence of Microsomes

A concentrated methanolic solution of cilnidipine was continuously added using a syringe pump (Harvard Apparatus, Holliston, MA) at a rate of 80  $\mu\text{L}/\text{min}$  to a solution of 100 mM pH 7.4 sodium phosphate buffer at a temperature of  $37 \pm 1^\circ\text{C}$  with constant stirring at 300 rpm. The tests were conducted in the absence and in the presence of pre-suspended rat liver microsomes at a concentration of 0.25 mg/mL. The light scattering evolved as a result of the formation of drug-rich aggregates was monitored every 10 s at 450 nm (non-absorbing wavelength) using a 400 UV-Vis spectrophotometer (SI Photonics, Tucson, AZ) in conjunction with a 1-cm pathlength dip probe.

#### Partitioning of the Probe Compound in the Drug-Rich Aggregates

10  $\mu\text{M}$  of each probe compound was added (from a stock solution in methanol) to a solution of 100 mM pH 7.4 sodium phosphate buffer containing increasing amounts of cilnidipine with final concentrations ranging between 0 and 50  $\mu\text{M}$ , at  $37 \pm 1^\circ\text{C}$ , with constant stirring at 300 rpm. The solutions were then centrifuged to remove the drug-rich aggregates at a temperature of  $37^\circ\text{C}$  and a speed of 35,000 rpm ( $112,303\times g$ ) for 30 min on an Optima L-100 XP ultracentrifuge (Beckman Coulter, Brea, CA) and a SW 41 Ti swinging bucket rotor attachment (Beckman Coulter, Brea, CA). The supernatant was then analyzed by high pressure liquid chromatography

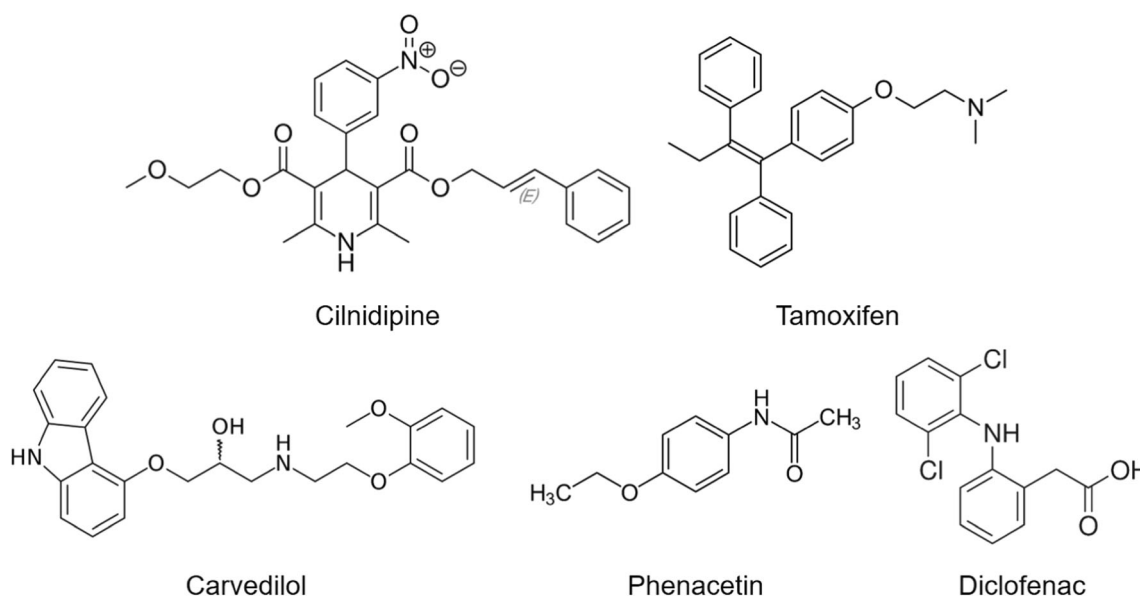


**Fig. 1** Chemical structures of the compounds used in this work.

(HPLC) using an Agilent 1100 HPLC system (Agilent Technologies, Santa Clara, CA) equipped with a Zorbax Eclipse Plus C18 analytical column ( $4.6 \times 150$  mm,  $5 \mu\text{m}$ ,  $95 \text{ \AA}$ ) (Agilent Technologies, Santa Clara, CA). The chromatographic conditions for each binary mixture can be seen in Table I. Standard solutions of the compounds in methanol-100 mM pH 7.4 sodium phosphate buffer 50/50 *v/v* were prepared to generate a calibration curve covering the concentration range of the compounds in the supernatant.

### *In Vitro* Metabolism Assays

Inhibition assays were performed for the following matrix substrate sets, phenacetin as a substrate with human liver microsomes (HLMs) and rCYP1A2, diclofenac with HLMs and rCYP2C9, tamoxifen with HLMs, rCYP2D6, rCYP2J2, and rCYP3A4, and carvedilol with HLMs, rCYP1A2, and rCYP2D6 in the following manner. Human liver microsomes or the relevant recombinant enzyme (final concentration 0.25 mg/mL) in 100 mM sodium phosphate buffer with various concentrations of cilnidipine (final concentrations 50, 25, 12.5, 6.5, 3.2, 1.6, 0.8  $\mu\text{M}$ ) and a vehicle (solvent) control were preincubated for 3 min at  $37^\circ\text{C}$ . The reaction was initiated by the addition of solution of NADPH (1 mM final concentration) and the individual substrates (final concentration 0.1  $\mu\text{M}$ ). After an incubation of 2, 6, 15, 30 and 60 min, the reaction was terminated by removing a 50  $\mu\text{L}$  aliquot of the incubation and adding to 100  $\mu\text{L}$  of a quench. After quenching the reaction, the mixture was centrifuged at approximately 4000 rpm for 10 min at room temperature. Following centrifugation the samples were analyzed via LC/MS/MS. Analytes and LC/MS/MS conditions are found in Table II.

Depletion rate constants ( $k$ ;  $\text{min}^{-1}$ ) were determined by calculating the slope from time (minutes) and natural log ( $\ln$ ) % of control remaining data for each of the substrate/inhibitor concentration/matrix sets.

$$\begin{aligned} \text{CL}_{\text{int}} &= k \left( \text{min}^{-1} \right) * 1000 \mu\text{L}/\text{mL} * (\text{mg microsomal protein}/\text{mL})^{-1} \\ &= \mu\text{L} * \text{min}^{-1} * \text{mg}^{-1} \end{aligned} \quad (1)$$

### Fitting of IC<sub>50</sub> Values

$\text{CL}_{\text{int}}$  values were normalized to vehicle control (100% activity). Each resulting % activity was plotted *versus* the log value of the respective inhibitor concentration and fitted to four  $\text{IC}_{50}$  models using Graphpad Prism v7.

$$\begin{aligned} \% \text{activity remaining} &= \\ & \frac{\text{Bottom} + (\text{Top} - \text{Bottom})}{1 + ((\text{inhibitor concentration}^{\text{Slope}})/(\text{IC}_{50}^{\text{Slope}}))} \end{aligned} \quad (2)$$

### Recombinant CYP Phenotyping

To determine the CYPs involved in the metabolism of the substrates (tamoxifen, carvedilol, phenacetin, and diclofenac), supersomes containing human recombinant cytochrome P450s (rCYP1A2, rCYP2B6, rCYP2C8, rCYP2C9, rCYP2C19, rCYP2D6, rCYP2J2, rCYP3A4, rCYP3A5, and the vector) and human liver microsomes were incubated at a concentration of 0.25 mg/ml with 0.1  $\mu\text{M}$  of the substrates (tamoxifen, carvedilol, phenacetin, and diclofenac). A 0 min time-point sample was taken by removing an aliquot of the incubation and adding to the quench; a small amount of

**Table I** Chromatographic Conditions Used for the Quantification of Cilnidipine and the Probe Compounds

System	Mobile phase	Flow rate (mL/min)	Injection volume ( $\mu\text{L}$ )	$\lambda_{\text{detection}}$ (nm)	Column temperature ( $^{\circ}\text{C}$ )
Cilnidipine-tamoxifen	20:80 pH 2.5 phosphoric acid water:acetonitrile	1	50	240	25
Cilnidipine-carvedilol	60:40 pH 2.5 phosphoric acid water:acetonitrile*	1	50	242	25
Cilnidipine-phenacetin	50:50 water:acetonitrile**	1	50	240	25
Cilnidipine-diclofenac	40:60 pH 2.5 phosphoric acid water:methanol***	1	50	230	25

\*Gradient: 0–3.5 min 60:40; 3.5–3.6 min 20:80; 3.6–8 min 20:80; 8–8.1 min 60:40; 8.1–10 min 60:40

\*\*Gradient: 0–3 min 50:50; 3–3.1 min 20:80; 3.1–7.2 min 20:80; 7.2–7.3 min 50:50; 7.3–9.2 min 50:50

\*\*\*Gradient: 0–1 min 40:60; 1–1.1 min 20:80; 1.1–8 min 20:80; 8–8.1 min 40:60; 8.1–10 min 40:60

NADPH was added to the quenched protein sample to normalize it. The CYP reaction was initiated by adding NADPH (final concentration of 1 mM) to the sample containing the matrix and the compound, followed by mixing. Time-points were taken at 5, 10, 25, 60, and 120 min by removing samples, adding to the quench and mixing. Depletion rate constants ( $k$ ;  $\text{min}^{-1}$ ) and intrinsic clearances ( $\mu\text{L}\cdot\text{min}^{-1}\cdot\text{mg}$ ) were determined as above (Eq. 1). rCYP  $\text{CL}_{\text{int}}$  values for the individual enzymes were further transformed to  $\mu\text{L}\cdot\text{min}^{-1}\cdot\text{pmol CYP}^{-1}$  using lot-specific rCYP content ( $\text{pmol}\cdot\text{mg protein}^{-1}$ ). The rCYP  $\text{CL}_{\text{int}}$  was used to predict a scaled HLM  $\text{CL}_{\text{int}}$  from each rCYP (Eq. 3) using an individual CYP relative activity factor (RAF) which

accounts for differences in probe CYP substrate  $\text{CL}_{\text{int}}$  for each of these liver and recombinant microsomal matrices (22).

$$\text{Scaled HLM } \text{CL}_{\text{int}} (\mu\text{L}\cdot\text{min}^{-1}\cdot\text{mg}^{-1}) = r\text{CYP}_x \text{CL}_{\text{int}} (\mu\text{L}\cdot\text{min}^{-1}\cdot\text{pmol}^{-1}) \cdot \text{RAF} (\text{pmol } r\text{CYP}_x \cdot \text{mg}^{-1}) \quad (3)$$

The fraction metabolized by a particular CYP (fm CYP<sub>x</sub>) as compared to total CYP mediated metabolism is determined by the ratio of HLM  $\text{CL}_{\text{int}}$  CYP<sub>x</sub> for an individual CYP to the sum of all HLM  $\text{CL}_{\text{int}}$  CYP<sub>x</sub> generated in the study (Eq. 4).

$$\text{fm CYP}_x = \text{Scaled HLM } \text{CL}_{\text{int}} \text{ CYP}_x / \sum \text{HLM } \text{CL}_{\text{int}} \text{ All CYP}_x \quad (4)$$

**Table II** Chromatographic Conditions used for the Quantification of Cilnidipine and the Probe Substrates by LC/MS/MS in the Metabolism Assays

Probe Substrate	Analyte	Transition (Da)	I.S.	Transition (Da)	Column	Mobile phase A	Mobile phase B	Injection volume ( $\mu\text{L}$ )
Phenacetin	Acetaminophen	152.10/110.10	Acetaminophen D4	156.10/114.10	Aquasil C18 2x20mm, 5 $\mu\text{m}$	H <sub>2</sub> O/Formic acid (1000:1 v/v)	MeOH	10
Bufuralol	Hydroxybufuralol	278.10/186.10	Hydroxybufuralol D9	287.10/186.10	Betasil C18 2 x 20 mm, 5 $\mu\text{m}$	H <sub>2</sub> O/2 M NH <sub>4</sub> HCO <sub>3</sub> (2000:50 v/v)	MeOH/2 M NH <sub>4</sub> HCO <sub>3</sub> (2000:50 v/v)	10
Diclofenac	4-Hydroxydiclofenac	312.10/229.90	4-Hydroxydiclofenac D6	318.00/236.00	Betasil C18 2 x 20 mm, 5 $\mu\text{m}$	H <sub>2</sub> O/2 M NH <sub>4</sub> HCO <sub>3</sub> (2000:50 v/v)	MeOH/2 M NH <sub>4</sub> HCO <sub>3</sub> (2000:50 v/v)	10
	Cilnidipine	494.30/117.10	LSNXXXXX187	305.20/148.10	Betasil C18 2 x 20 mm, 5 $\mu\text{m}$	H <sub>2</sub> O/2 M NH <sub>4</sub> HCO <sub>3</sub> (1000:25 v/v)	Acetonitrile	10
	Tamoxifen	372.20/72.10	LSNXXXXX189	333.20/148.10	Betasil C18 2 x 20 mm, 5 $\mu\text{m}$	H <sub>2</sub> O/2 M NH <sub>4</sub> HCO <sub>3</sub> (1000:25 v/v)	Acetonitrile	10

## RESULTS AND DISCUSSION

### Formation of Drug-Rich Aggregates in Solutions Containing Microsomes

Determination of the onset concentration for the formation of drug-rich cilnidipine aggregates in the presence of microsomes was achieved using light scattering. This approach can be carried out in the presence of a strong scatterer/absorbing species such as the microsomes by blanking the microsomes solution and measuring the extinction of light as a result of scattering following the formation of drug-rich aggregates. The evolution of the scattering at a nonabsorbing wavelength (450 nm) as a function of the cilnidipine concentration in the absence and presence of the microsomes is shown in Fig. 2. In the absence of microsomes, the extinction increases after reaching a cilnidipine concentration of  $\sim 4 \mu\text{M}$  (Fig. 2a), while in the presence of microsomes, the concentration of cilnidipine required to give an increase in scattering is  $\sim 8 \mu\text{M}$  (Fig. 2b). It is apparent that the concentration for the formation of drug-rich cilnidipine aggregates increases in the presence of microsomes, and this is due to the drug interacting with the proteins and lipids forming the microsomes, which in turn reduces the free drug concentration, requiring higher total concentrations to induce aggregate formation. A similar increase in the presence of microsomes has been also described for the calcium channel antagonist, felodipine (23).

### Partitioning of the Probe Compound into the Drug-Rich Aggregates

To obtain information on the partitioning of the probe compound into the drug-rich aggregates, a series of solutions containing a fixed concentration of probe compound and increasing concentrations of cilnidipine were prepared, ultracentrifuged to pellet the drug-rich aggregates and the amount of each compound in the supernatant was determined using HPLC.

It is anticipated that if partitioning does not occur, the concentration of the probe compound in the supernatant will be the same as the amount added to the solution. In contrast, if partitioning occurs, the probe compound will be depleted from the supernatant due to pelletization of a fraction of the probe molecules with the drug-rich aggregates. The extent of sequestration is expected to depend on the amount of the drug-rich aggregates, and the ability of probe molecule to mix with the aggregate-forming compound.

The concentration in the supernatant of each component as a function of added cilnidipine is shown in Fig. 3. Starting with the cilnidipine-tamoxifen system (Fig. 3a), it can be seen that the concentration of cilnidipine begins to plateau after exceeding  $\sim 1 \mu\text{M}$ , which is consistent with the formation of drug-rich aggregates, and the tamoxifen concentration

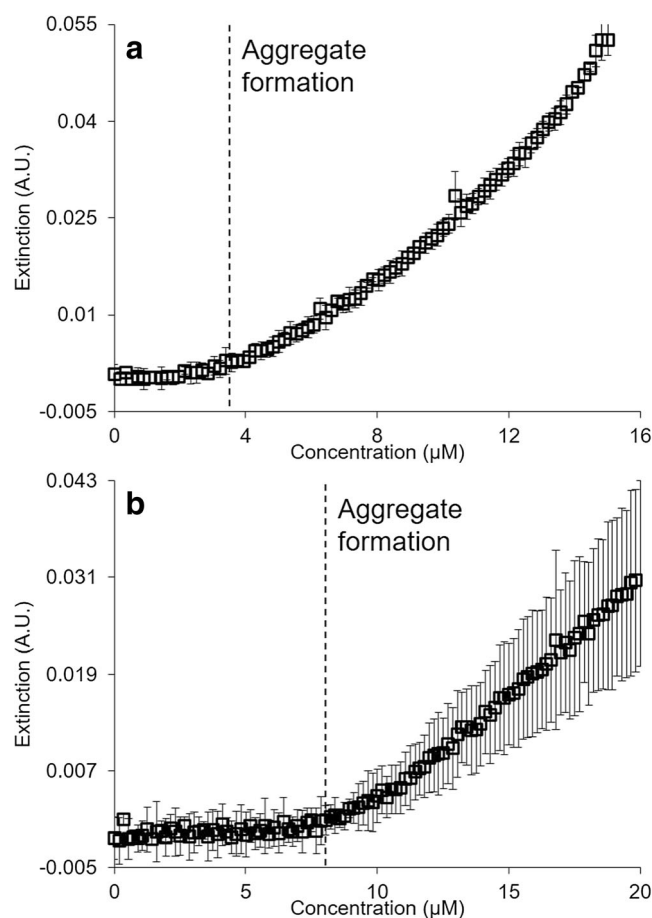


**Fig. 2** Evolution of UV extinction at 450 nm (mean of two measurements, error bars show range) of cilnidipine (a) in the absence and (b) in the presence of liver microsomes.

substantially decreases from  $\sim 5 \mu\text{M}$  to  $\sim 2 \mu\text{M}$ . This indicates that the concentration of tamoxifen in solution is reduced due to sequestration by the drug-rich cilnidipine aggregates.

Turning now to carvedilol (Fig. 3b), phenacetin (Fig. 3c) and diclofenac (Fig. 3d), we note that the supernatant concentration of each probe compound is equivalent to the amount added to the solution, even in the presence of high amounts of cilnidipine aggregates. This demonstrates that no detectable mixing occurs between these compounds and the cilnidipine aggregates.

Of all of the probe compounds evaluated, only tamoxifen showed mixing with the cilnidipine aggregates, and this is likely due to its high hydrophobicity ( $\log P$  of 6.6) (24) and thus high affinity for the lipophilic aggregates. Phenacetin is characterized by a low hydrophobicity ( $\log P$  of 1.6) (25) and this would explain the lack of affinity and mixing with the aggregates. Carvedilol and diclofenac did not mix with the aggregates as they are both in the ionized form at pH 7.4 due to their weakly basic (carvedilol  $pK_a$  is 7.8) (26) and weakly acidic (diclofenac  $pK_a$  is 4.2) (18) nature. Ionized compounds are not expected to interact with lipophilic aggregates.

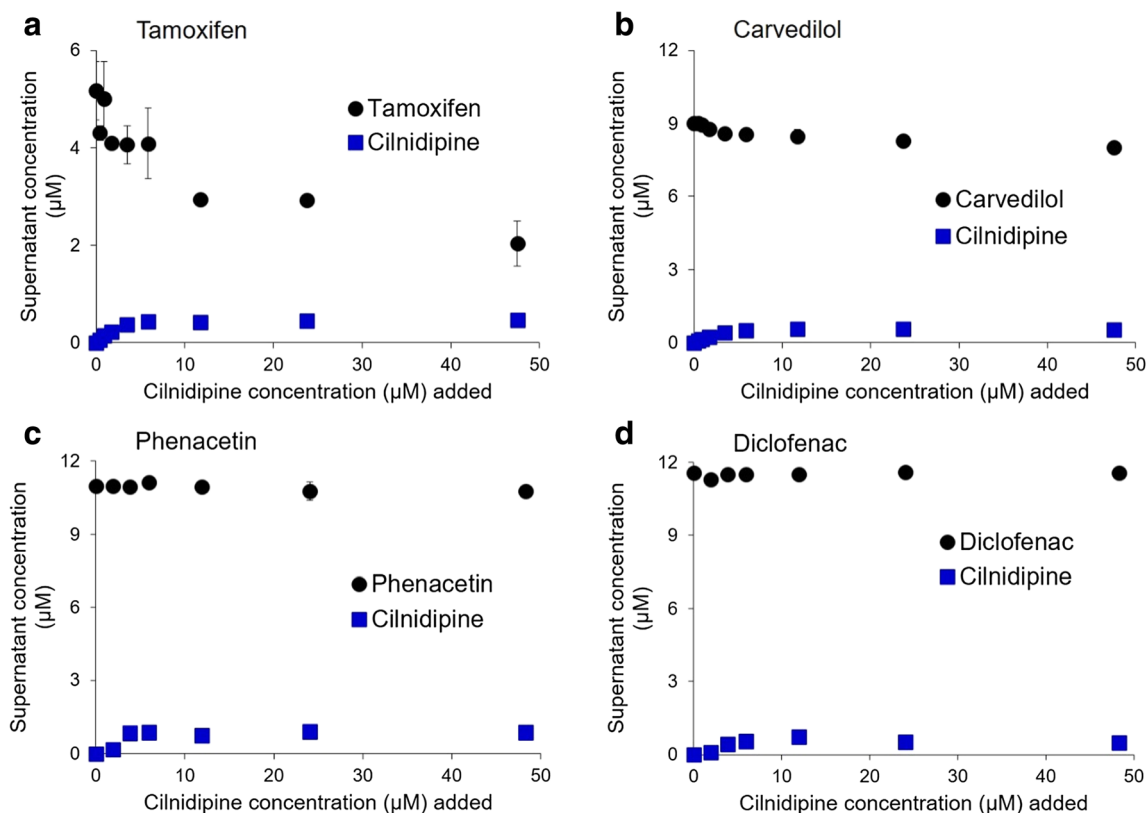


**Fig. 3** Impact of increasing amounts of drug-rich cilnidipine aggregates on the bulk solution concentration of (a) tamoxifen, (b) carvedilol, (c) phenacetin and (d) diclofenac. The bulk solution concentration of cilnidipine is also shown.

### *In Vitro* Metabolism Assays

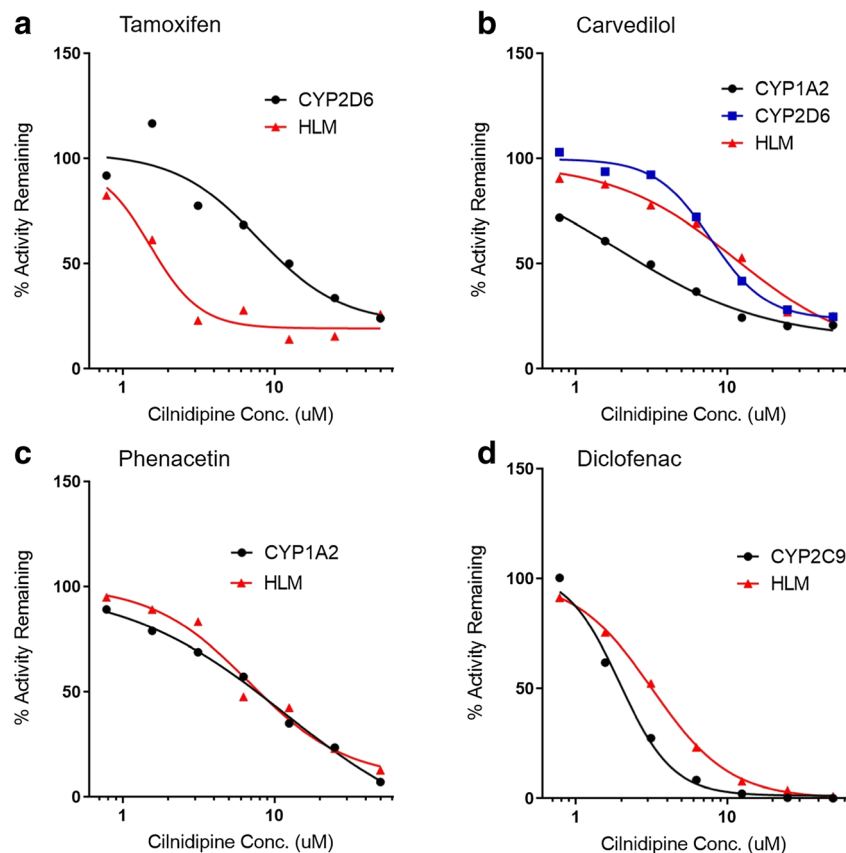
The effect of cilnidipine aggregates on the metabolism of the probe compounds (tamoxifen, carvedilol, phenacetin and diclofenac) was studied in HLMs and various recombinant CYP enzymes. The % activity remaining (compared to vehicle control) for each enzymatic system *vs* the cilnidipine concentration for the various probe compounds and fit to a four parameter sigmoidal model is presented in Fig. 4.

Starting with the tamoxifen data (Fig. 4a), it can be seen that, in the presence of low cilnidipine concentrations, the metabolism of the probe compound by the enzymes is minimally affected. However, at higher concentrations where cilnidipine is present as aggregates, there is a progressive decrease in the rate of metabolism with only 24% and 26% of activity remaining for rCYP2D6 and HLM, respectively, at a cilnidipine concentration of 50 μM (Fig. 4). Thus, cilnidipine potently inhibits the tamoxifen metabolism, which cannot be readily explained based on structural considerations. Cilnidipine is a neutral compound with a large and non-planar structure and is not a substrate/inhibitor of CYP2D6, which metabolizes medium size basic amines. A CYP phenotyping assay of cilnidipine with rCYP2D6 confirmed no turnover of cilnidipine by the enzyme. One potential explanation for the observed behavior is that, as described above (Fig. 3a), tamoxifen partitions into the cilnidipine

aggregates, reducing the free drug concentration available for interaction with the enzyme. As more of the substrate molecules become entrapped in the aggregates, the apparent affinity of the substrate for the enzyme decreases and thus the rate of metabolism appears inhibited.

Turning now to the metabolism data for carvedilol (Fig. 4b), phenacetin (Fig. 4c) and diclofenac (Fig. 4d), we note that, similarly to tamoxifen, the intrinsic clearance of these substrates is drastically reduced in the presence of high amounts of cilnidipine aggregates such that the % activity remaining at a cilnidipine concentration of 50 μM is 21% (rCYP1A2) and 25% (rCYP2D6 and HLM) for carvedilol, 7% (rCYP1A2) and 13% (HLM) for phenacetin, and 0.1% (rCYP2C9) and 1% (HLM) for diclofenac. Again, this pattern of inhibition cannot be explained based on structural considerations. Cilnidipine is a neutral compound characterized by a large and non-planar structure and was not a substrate of rCYP2D6, rCYP1A2 and rCYP2C9 with no apparent substrate loss with incubation with any of the recombinant CYP enzymes. As the apparent affinity of these substrates for the enzymes does not change, and it was previously shown that the free concentration of these substrates is not reduced in the presence of drug-rich cilnidipine aggregates (Fig. 3b, c and d), it is likely that the cilnidipine aggregates directly interfere with the enzymes present in the membranes, leading to the observed loss of activity. This is a non-specific effect that

**Fig. 4** Effect of drug-rich cilnidipine aggregates on (a) CYP2D6 and HLM with tamoxifen as a substrate, (b) CYP1A2, CYP2D6 and HLM with carvedilol as a substrate, (c) CYP1A2 and HLM with phenacetin as a substrate and (d) CYP2C9 and HLM with diclofenac as a substrate.



manifests as inhibition of multiple enzymes, i.e., rCYP2D6, rCYP1A2 and rCYP2C9. The non-specific effect would explain the differences in inhibition potency observed for tamoxifen (HLM *vs* rCYP2D6) and carvedilol (rCYP1A2 *vs* HLM and rCYP2D6). The inhibition of various recombinant CYPs with very different active sites (e.g., rCYP2D6 and rCYP2C9) is evidence that the drug-rich aggregates may interact outside the active site, possibly leading to partial denaturation of the proteins. Aggregates have been previously shown to non-specifically inhibit soluble enzymes by sequestration and partial denaturation (8,14).

The concentration of cilnidipine where the activity of the enzymes is reduced by half, i.e.,  $IC_{50}$ , was calculated for each substrate/enzyme system and the values obtained are summarized in Table III. As calculating an  $IC_{50}$  would infer that cilnidipine may be behaving as a competitive inhibitor, which is not the case based on the data, the term promiscuous  $IC_{50}$  is

used here to distinguish the non-specific promiscuous aggregation based inhibition from a specific competitive inhibition mechanism. The data in Table III indicate that the cilnidipine aggregates non-specifically inhibit rCYP2D6, rCYP1A2, rCYP2C9 and the HLM with a promiscuous  $IC_{50} < 12.5 \mu M$  for all the systems investigated. These values are comparable with the  $IC_{50}$  values of potent model inhibitors such as mefenamic acid ( $IC_{50} = 3.4 \mu M$ , CYP1A2) (27) and rofecoxib ( $IC_{50} = 8.7 \mu M$ , CYP1A2) (27), highlighting that the extent of inhibition caused by the drug-rich aggregates is significant.

The phenomenon of promiscuous aggregation can lead to false positives during *in vitro* assays as aggregates non-specifically but potentially inhibit the activity of metabolic enzymes, leading to an inappropriate *in vivo* prediction of potential clinical drug-drug interactions. For instance, it was shown herein that cilnidipine inhibited the metabolism of

**Table III** Inhibition of rCYP2D6, rCYP1A2, rCYP2C9 and HLM by Cilnidipine Aggregates

Compound	Non-specific $IC_{50}$ vs rCYP2D6 ( $\mu M$ )	Non-specific $IC_{50}$ vs rCYP1A2 ( $\mu M$ )	Non-specific $IC_{50}$ vs CYP2C9 ( $\mu M$ )	Non-specific $IC_{50}$ vs HLM ( $\mu M$ )
Tamoxifen	7.56	NA	NA	1.75
Carvedilol	7.82	3.26	NA	10.9
Phenacetin	NA	12.5	NA	6.77
Diclofenac	NA	NA	1.44	3.27

carvedilol mediated by rCYP1A2, although it is not a substrate/competitive inhibitor of this enzyme. This is an artifact that results in incorrect predictions of *in vivo* drug-drug interactions between these two compounds. Based on the data shown herein, all *in vitro* data should be considered before *in vivo* effects are predicted. It is unlikely that compounds will reach the free concentrations at which these aggregates form (concentrations of  $\mu\text{M}$  order) in the systemic circulation and intracellularly in hepatocytes, however, enzymes and transporters at the intestinal wall often encounter these very high concentrations and possible enzyme/transporter inhibition mediated by the aggregates could lead to promiscuous inhibition *in vivo*. In this paradigm, important *in vitro* artifacts caused by the drug-rich aggregates may translate into a previously unrecognized mode of *in vivo* drug-drug interactions.

## CONCLUSIONS

The impact of drug-rich aggregates on *in vitro* drug metabolism assays was successfully demonstrated. This was achieved by measuring the activity of rCYP2D6, rCYP1A2, rCYP2C9 enzymes and HLM in the presence of cilnidipine aggregates. It was found that the drug-rich aggregates inhibited multiple enzymes in a non-specific way with a promiscuous  $\text{IC}_{50}$  comparable to the  $\text{IC}_{50}$  values of potent model inhibitors. The “promiscuous inhibition” mode was attributed to the aggregates directly interfering with/denaturing the enzymes as well as sequestering highly hydrophobic substrates (e.g., tamoxifen) and thus reducing their apparent affinity for the enzyme. Based on the observations presented herein, compounds that form drug-rich aggregates can lead to artefacts during *in vitro* metabolism assays and erroneous conclusions about drug-drug interactions. Thus, the “promiscuous inhibition” mode needs to be taken into account in the future to achieve a more appropriate prediction of *in vivo* performance.

## ACKNOWLEDGMENTS

The authors wish to acknowledge Eli Lilly and Co. for funding through the LRAP program.

## REFERENCES

- Galetin A, Gertz M, Houston JB. Potential role of intestinal first-pass metabolism in the prediction of drug–drug interactions. *Expert Opin Drug Metab Toxicol*. 2008;4(7):909–22. <https://doi.org/10.1517/17425255.4.7.909>.
- Bjornsson TD, Callaghan JT, Einolf HJ, Fischer V, Gan L, Grimm S, et al. The conduct of in vitro and in vivo drug-drug interaction studies: a PhRMA perspective. *J Clin Pharmacol*. 2003;43(5):443–69. <https://doi.org/10.1177/0091270003252519>.
- Mao J, Mohutsky MA, Harrelson JP, Wrighton SA, Hall SD. Prediction of CYP3A-mediated drug-drug interactions using human hepatocytes suspended in human plasma. *Drug Metab Dispos*. 2011;39(4):591 LP–602.
- Xu L, Chen Y, Pan Y, Skiles GL, Shou M. Prediction of human drug-drug interactions from time-dependent inactivation of CYP3A4 in primary hepatocytes using a population-based simulator. *Drug Metab Dispos*. 2009;37(12):2330 LP–2339.
- Feng BY, Simeonov A, Jadhav A, Babaoglu K, Ingles J, Shoichet BK, et al. A high-throughput screen for aggregation-based inhibition in a large compound library. *J Med Chem*. 2007;50(10):2385–90. <https://doi.org/10.1021/jm061317y>.
- McGovern SL, Caselli E, Grigorieff N, Shoichet BK. A common mechanism underlying promiscuous inhibitors from virtual and high-throughput screening. *J Med Chem*. 2002;45(8):1712–22. <https://doi.org/10.1021/jm010533y>.
- McGovern SL, Helfand BT, Feng B, Shoichet BK. A specific mechanism of nonspecific inhibition. *J Med Chem*. 2003;46(20):4265–72. <https://doi.org/10.1021/jm030266r>.
- Seidler J, McGovern SL, Doman TN, Shoichet BK. Identification and prediction of promiscuous aggregating inhibitors among known drugs. *J Med Chem*. 2003;46(21):4477–86. <https://doi.org/10.1021/jm030191r>.
- Feng BY, Shelat A, Doman TN, Guy RK, Shoichet BK. High-throughput assays for promiscuous inhibitors. *Nat Chem Biol*. 2005;1:146.
- Feng BY, Shoichet BK. A detergent-based assay for the detection of promiscuous inhibitors. *Nat Protoc*. 2006;1(2):550–3. <https://doi.org/10.1038/nprot.2006.77>.
- Coan KED, Shoichet BK. Stoichiometry and physical chemistry of promiscuous aggregate-based inhibitors. *J Am Chem Soc*. 2008;130(29):9606–12. <https://doi.org/10.1021/ja802977h>.
- Doak AK, Wille H, Prusiner SB, Shoichet BK. Colloid formation by drugs in simulated intestinal fluid. *J Med Chem*. 2010;53(10):4259–65. <https://doi.org/10.1021/jm100254w>.
- Coan KED, Maltby DA, Burlingame AL, Shoichet BK. Promiscuous aggregate-based inhibitors promote enzyme unfolding. *J Med Chem*. 2009;52(7):2067–75. <https://doi.org/10.1021/jm801605r>.
- Sassano MF, Doak AK, Roth BL, Shoichet BK. Colloidal aggregation causes inhibition of G protein-coupled receptors. *J Med Chem*. 2013;56(6):2406–14. <https://doi.org/10.1021/jm301749y>.
- Owen SC, Doak AK, Wassam P, Shoichet MS, Shoichet BK. Colloidal aggregation affects the efficacy of anticancer drugs in cell culture. *ACS Chem Biol*. 2012;7:1429–35.
- Kirchmair J, Göller AH, Lang D, Kunze J, Testa B, Wilson ID, et al. Predicting drug metabolism: experiment and/or computation? *Nat Rev Drug Discov*. 2015;14:387.
- Trasi NS, Taylor LS. Thermodynamics of highly supersaturated aqueous solutions of poorly water-soluble drugs - impact of a second drug on the solution Phase behavior and implications for combination products. *J Pharm Sci*. 2015;104(8):2583–93. <https://doi.org/10.1002/jps.24528>.
- Alhalaweh A, Bergström CAS, Taylor LS. Compromised in vitro dissolution and membrane transport of multidrug amorphous formulations. *J Control Release*. 2016;229:172–82. <https://doi.org/10.1016/j.jconrel.2016.03.028>.
- Lindfors L, Forssén S, Skantze P, Skantze U, Zackrisson A, Olsson U. Amorphous drug nanosuspensions. 2. Experimental determination of bulk monomer concentrations. *Langmuir*. 2006;22(3):911–6. <https://doi.org/10.1021/la052367t>.



21. Raina SA, Alonzo DE, Zhang GGZ, Gao Y, Taylor LS. Using environment-sensitive fluorescent probes to characterize liquid-liquid phase separation in supersaturated solutions of poorly water soluble compounds. *Pharm Res*. 2015;32(11):3660–73. <https://doi.org/10.1007/s11095-015-1725-z>.
22. Emoto C, Iwasaki K. Approach to predict the contribution of cytochrome P450 enzymes to drug metabolism in the early drug-discovery stage: the effect of the expression of cytochrome B5 with recombinant P450 enzymes. *Xenobiotica*. 2007;37(9):986–99. <https://doi.org/10.1080/00498250701620692>.
23. Tres F, Hall SD, Mohutsky MA, Taylor LS. Monitoring the phase behavior of supersaturated solutions of poorly water-soluble drugs using fluorescence techniques. *J Pharm Sci*. 2018;107(1):94–102.
24. Simpson NJ, Solid-Phase K. *Extraction: principles, techniques, and applications*. Marcel Dekker, Inc: New York; 2000.
25. Baird JA, Van Eerdenbrugh B, Taylor LS. A classification system to assess the crystallization tendency of organic molecules from under-cooled melts. *J Pharm Sci*. 2010;99(9):3787–806. <https://doi.org/10.1002/jps.22197>.
26. Loftsson T, Vogensen SB, Desbos C, Jansook P. Carvedilol: solubilization and cyclodextrin complexation: a technical note. *AAPS PharmSciTech*. 2008;9(2):425–30. <https://doi.org/10.1208/s12249-008-9055-7>.
27. Karjalainen MJ, Neuvonen PJ, Backman JT. In vitro inhibition of CYP1A2 by model inhibitors, anti-inflammatory analgesics and female sex steroids: predictability of in vivo interactions. *Basic Clin Pharmacol Toxicol*. 2008;103(2):157–65. <https://doi.org/10.1111/j.1742-7843.2008.00252.x>.

**Publisher's Note** Springer Nature remains neutral with regard to jurisdictional claims in published maps and institutional affiliations.